NPRC Journal of Multidisciplinary Research
Volume 3, Issue 7, July, 2026 Pages: 17-38
ISSN: 3059-9148 (Online)
DOI: 10.3126/nprcjmr.v3i7.95540

Field Calibration of Non-Destructive Testing for Post-Fire Residual Strength of Reinforced Concrete

Sarun Bhomi*
Institute of Engineering, Pulchowk Campus,
Tribhuvan University, Lalitpur, Nepal
079mscom020.sarun@pcampus.edu.np
https://orcid.org/0009-0000-9887-9954

Kushal Bhandari
Institute of Engineering, Pulchowk Campus,
Tribhuvan University, Lalitpur, Nepal
072bce074.kushal@pcampus.edu.np
https://orcid.org/0009-0001-4867-7390

Corresponding Author*
Received: May 22, 2026 Revised & Accepted: July 25, 2026

Abstract

Background: Non-destructive testing (NDT) using Ultrasonic Pulse Velocity (UPV) and Rebound Hammer (RN) is widely used for post-fire concrete assessment, but standard calibrations derived from laboratory specimens are unreliable under field conditions. A further challenge arises when a fire-damaged building contains multiple concrete grades (e.g., M20 and M25).

Objective: This study recalibrates single-method and combined (SonReb) NDT equations using field data from real fire-damaged buildings, tests whether M20 and M25 share a common NDT- strength slope, and quantifies between-building variability.

Methods: UPV, RN, and destructive core tests were conducted on 81 members (beams, slabs, columns) across 13 fire-damaged government buildings in Nepal (M20: n=64; M25: n=17). Calibrations were derived at pooled, M20, and M25 levels using ordinary least squares, evaluated with leave-one-out cross-validation (R^2_{LOOCV}), and tested for slope equality via interaction terms. Between-building variance was partitioned using Intra Class Correlation (ICC).

Results: UPV (r=0.64) and RN (r=0.72) correlated with core strength. Slope-equality tests showed no significant grade interaction (p≥0.79), supporting a common slope with grade-specific intercepts. However, the M25 RN model failed cross-validation (R2LOOCV=−0.12). The M20 SonReb model performed best (R^2_{LOOCV}=0.60; RMSE=4.49 MPa). Between-building differences explained 63% of strength variation (ICC=0.63).
Conclusion: NDT is suitable for comparative ranking of fire-damaged members but not for absolute strength estimation without site-specific recalibration using a limited number of destructive cores. The common-slope, grade-intercept approach is statistically defensible for mixed-grade buildings.
Keywords: Concrete, Fire damage, Non-destructive testing, Rebound hammer, Residual strength, SonReb, UPV

1. Introduction

Fire is one of the most devastating accidents for a Reinforced Concrete (RC) structure. Elevated temperatures can cause a range of changes in chemical and physical composition in the cement-paste matrix, including dehydration of the calcium silicate hydrate gel and decomposition of calcium hydroxide which can substantially degrade some properties of concrete (Caetano et al., 2019; Khoury, 2000). The resulting loss of strength is a primary factor that determines whether a structure that is exposed to fire damage can be safely reoccupied, repaired, or must be demolished. Therefore, a rapid and reliable estimation of residual compressive strength is important for conducting post-fire analysis of structures (Pasztetnik & Wróblewski, 2021; Qin et al., 2022).

Ultrasonic pulse velocity (UPV) and the rebound hammer remain the most useful and convenient way of post-fire structural assessment. They are widely use because of their rapid, inexpensive, and non-invasive working mechanisms (Bungey et al., 2006; Wróblewska & Kowalski, 2020). UPV reflects the bulk elastic modulus and internal microcracking along the transmission path, whereas the rebound number (RN) indexes near-surface hardness. Both methods are present in IS 13311 Parts 1 and 2 (Bureau of Indian Standards, 1992a, 1992b), which provide uniform classification thresholds for field application. Furthermore, Combined-method approaches such as SonReb (joint use of UPV and RN) have been proposed to improve in-situ strength estimation in undamaged and aged structures. There is also reported improvements whenever this method is used for cross-validated agreement (El-Mir et al., 2023).

One consistent finding across the NDT-to-strength literature is that no universal formula exists(Rashid & Waqas, 2017). Calibrations published over the past two decades vary widely in their mathematical form, and their slope and intercept values differ substantially. It also differs by the types of concrete they were developed for, laboratory cubes and cores taken from site.

Site-specific recalibration is therefore an accepted requirement of NDT practice (Choi et al., 2021; Pucinotti, 2015; Wróblewska & Kowalski, 2020). For engineers the challenge is not only the formula to apply, but to build a reliable calibration that is specific to the structure being assessed. In a fire-damaged structure containing more than one concrete grade, an important question is whether a single pooled calibration is sufficient or whether grade-stratified equations should be fitted separately. This is important because a single combined calibration is simpler to apply but may mask differences in behaviour between concrete grades, whereas separate calibrations for each grade are more informative but require a larger number of cores to be statistically reliable

The contribution of this study is empirical and quantitative. We assembled UPV, rebound, and destructive core data on 81 members from 13 fire-damaged RC buildings across various fire-damaged government buildings of Nepal due to GEN-Z protests. The study covers a wide range of fire severities, including both M20 and M25 concrete in beams, slabs, and columns.

The specific objectives are:

1. To quantify the correlation between UPV and rebound hammer readings and destructive core strength under real fire-damage field conditions, and to determine whether standard NDT codes reliably estimate residual strength in fire-damaged elements;
2. To derive field-recalibrated single-method (UPV and RN) and combined SonReb strength equations at pooled, M20, and M25 grade levels, evaluated through leave-one-out cross-validation and reported with confidence intervals;
3. To formally test whether the NDT–strength slope differs between M20 and M25 concrete grades, and thereby determine whether a shared slope with grade-specific intercepts constitutes a statistically defensible calibration strategy for mixed-grade structures;
4. To quantify the proportion of residual strength variation attributable to between-building differences using random-effects variance partitioning, and to assess its implications for transferring calibration equations across fire events; and
5. To provide practical guidance on the sufficiency of NDT, and when building-specific recalibration against a limited set of destructive cores is required for absolute strength estimation.

2. Background and Literature Review

2.1. Fire effects on concrete

The mechanical response of concrete to high temperature comprises a sequence of physico-chemical changes in the cement-paste matrix and the aggregate (Kodur, 2014). Below about 300 °C, the loss of evaporable and chemically bound water happens, which reduces stiffness and initiates microcracking. In the temperature range between 300 °C and 600 °C, decomposition of the calcium silicate hydrate gel and the conversion of portlandite to calcium oxide weaken the paste irreversibly (Miao et al., 2026). As temperature approaches and exceeds 600 °C, aggregate stability becomes the primary determinant of residual composite integrity. At 573°C, standard α quartz undergoes disruptive crystal structure transformation into β quartz, inducing volume instability and internal microcracking that damage ordinary aggregates from the inside out (Rovnanik, 2015).

NPRC Journal of Multidisciplinary Research
Volume 3, Issue 7, July, 2026 Pages: 17-38
ISSN: 3059-9148 (Online)
DOI: 10.3126/nprcjmr.v3i7.95540

In denser, lower-permeability concretes, water trapped in the pores cannot escape fast enough, and the resulting steam pressure can cause sudden, explosive spalling of the concrete surface(Caetano et al., 2019; Khoury, 2000). The overall process is not a simple monotonic decay. Recent experiments show that residual strength depends not only on the peak temperature reached but also on how the concrete cools and what moisture it sees after the fire; also, these factors can shift the remaining strength by tens of percentage(Kodur & Agrawal, 2016; Pasztetnik & Wróblewski, 2021).

The concrete grade also matters. Higher-strength concretes have a denser pore structure and let less water move through them. This works in their favour after moderate heating, because the tighter matrix holds onto more of its original strength. But it works against them at higher temperatures at around 200 °C to 400 °C where the water trapped inside the pores turns to steam and cannot escape quickly enough, and the pressure that builds up can crack or spall the surface.(Agrawal & Kodur, 2020; Elsanadedy, 2019). Recent comprehensive reviews of post-fire RC assessment find that the residual mechanical response of a fire-exposed member cannot be predicted from temperature alone and must be measured (Concrete Society, 2008; Qin et al., 2022).

2.2. Ultrasonic pulse velocity in fire-damaged concrete

In the case of normal concrete, UPV gives a fairly reliable indication of how stiff and dense the material is, but the readings for fire damaged concrete, the readings become difficult to interpret. Cracking, pore coarsening, and the loss of bound water result in a loss of velocity, but it happens at different temperatures and to different depths from the heated surface. Therefore, the bulk average velocity along a transmission path mixes signal from layers in radically different mechanical states (Wróblewska & Kowalski, 2020).

(Choi et al., 2021), working with concrete specimens exposed to controlled thermal treatments up to 800 °C, identified a robust correlation between residual UPV and compressive strength, proposing post-fire linear calibration equations. However, these thermal degradation models differ in their parameter baselines from conventional linear equations calibrated for undamaged concrete like that of (Qasrawi, 2000). This is a finding consistent with the broader observation that undamaged-concrete UPV-strength equations are not transferable to fire-damaged concrete without recalibration (Choi et al., 2021; Wróblewska & Kowalski, 2020).

Felicetti's research at Politecnico di Milano proposed NDT techniques designed specifically for fire-damaged concrete, including indirect UPV using refraction and drilling-resistance measurements. These methods can reliably determine how deep the heat damage has penetrated which solves the limitation of the standard single-measurement UPV test (Colombo & Felicetti, 2007; Felicetti, 2006) In practice, this means that UPV readings can help to identify where damage is worse or less severe but the actual strength of concrete data is unreliable. Addressing this limitation is precisely what this study aims to do.

2.3. Rebound hammer and SonReb combined-method approaches

The rebound hammer detects near-surface hardness and is sensitive to surface moisture, finish, aggregate type, and carbonation depth in addition to bulk strength (Bungey et al., 2006;

NPRC Journal of Multidisciplinary Research
Volume 3, Issue 7, July, 2026 Pages: 17-38
ISSN: 3059-9148 (Online)
DOI: 10.3126/nprcjmr.v3i7.95540

Kowalski & Wróblewska, 2018). In a post-fire context, these surface changes can lead to differences in interpretation. (Liu & Chen, 2022) demonstrates that at 400 °C, localised moisture trapping mechanisms can trigger secondary hydration of previously unhydrated cement particles, temporarily elevating strength though underlying concrete undergoes thermal degradation. Therefore, the rebound number can stay misleadingly high in a member whose bulk strength has fallen substantially (Kowalski & Wróblewska, 2018; Wróblewska & Kowalski, 2020).

Kowalski and Wróblewska's controlled laboratory study on RC beams heated for 60–240 minutes from one face confirmed that the rebound number of the heated face does not track residual strength reliably. This study recommended its use only as a preliminary screening tool and not for absolute strength estimation (Kowalski & Wróblewska, 2018) . Recent work has tried to resolve this problem with combined-method (SonReb) calibrations and machine-learning models that jointly use rebound and UPV inputs to predict strength (El-Mir et al., 2023). These approaches improve in-sample R^2 but have been validated almost entirely on undamaged or laboratory-heated specimens rather than on members from real fire events. The core problem with the rebound hammer is that it only measures the concrete surface. After a fire, the surface is the most damaged part and no longer reflects the true strength of the concrete which lies beneath. This is exactly why the standard rebound hammer formula cannot be trusted to give accurate strength values in fire-damaged concrete.

2.4. Absence of a transferable formula and the case for stratified field calibration

A review of various research regarding NDT-to-strength calibrations confirms a problem that there is no single universal equation. Qasrawi's (Qasrawi, 2000) linear UPV calibration is widely used as a default, but it was developed from undamaged, ordinary concrete in the 20–40 MPa range. Pucinotti's (Pucinotti, 2015) field study on a historic museum found that UPV gave reasonable results, but the rebound hammer performed poorly on its own, and produced different numbers than Qasrawi altogether. Also, Katuwal's (Katuwal, 2019) work on M20 concrete from the Pokhara Valley in Nepal found that simply changing the aggregate source was enough to shift the calibration, which means that even within the same concrete grade and the same region the equations are different. Even the widely used Proceq N-type manufacturer curve (Proceq, 2019) comes with a clear warning that it is only a starting point and must be verified for each specific project. This study asks a practical question regarding assessment of fire-damaged building that contains two different concrete grades and whether calibration for both grades together is suitable or separate ones for each.

2.5. Research gap

The relation between NDT and strengths available for fire-damaged concrete much derives from specimens heated in furnaces under controlled, uniform temperatures, and not from members subjected to the spatially uneven exposure of a real building fire. Calibrations which are related to destructive cores from actual fire events, and across more than a single structure is not studied which is one of the gaps this research is trying to cover .Secondly it is widely accepted that no transferable formula exists and that site-specific recalibration is unavoidable

NPRC Journal of Multidisciplinary Research
Volume 3, Issue 7, July, 2026 Pages: 17-38
ISSN: 3059-9148 (Online)
DOI: 10.3126/nprcjmr.v3i7.95540

(Choi et al., 2021; Pucinotti, 2015; Wróblewska & Kowalski, 2020), the literature is silent on how such recalibration should be structured when one structure contains more than one concrete grade. This research determines whether a single equation can reliably serve a real building comprising various strengths of concrete across different grades. Finally, SonReb combined-method equations have only ever been tested on the same data used to build them. No one has checked whether they actually hold up on new, independent data. This means engineers currently have no reliable evidence to help them decide whether to use one calibration for all concrete grades or separate calibrations for each.

This study fills these gaps by building calibration equations from 81 tested members across 13 fire-damaged buildings. It tests whether M20 and M25 concrete behave differently under NDT, and checks how well the equations perform on data. This gives engineers a reliable basis for deciding whether to use one equation for all grades or use separate for concrete of various strengths.

3. Materials and methods

3.1. Study Sites and Scope

The field testing was carried out for 13 reinforced concrete framed structures affected by fire damage, including both rural and urban settings in Nepal, across two areas: ten structures in the Banke district and three in Kathmandu district. In each building, the beams, slabs, and columns exposed to fire damage were first identified through visual observations, focusing on concrete spalling extent, reinforcement exposure, cracking patterns, deflections, and material discoloration as key indicators of thermal severity. Later destructive and non-destructive tests were conducted. All the tests were carried out by the trained personnel using the standardised instrumented inventory.

3.2. Test Programme and data inventory

Three testing methods via. Ultrasonic Pulse Velocity as per IS 13311 Part 1(Bureau of Indian Standards, 1992a), Rebound Hammer as per IS 13311 Part 2(Bureau of Indian Standards, 1992b), and Destructive Concrete Cores for Compressive Strength as per IS 516 Part 4(Bureau of Indian Standards, 2018) were conducted on every member. The dataset only comprises samples where all three testing techniques were carried out on each of the samples, resulting in 81 samples from 13 buildings (Table I). For each structural member, UPV was calculated as the ratio of the path length between two transducers and the transit time of the ultrasonic wave (V = L/T). Similarly, Rebound Number (RN) was calculated as the mean of a 16-point measurement grid subjected to outlier screening as per IS 13311 Part 2. Finally, core testing was done to determine equivalent cube compressive strengths calculated using the failure load using standard length-to-diameter and IS 516 correction factors.

***Table I**: Member counts by Concrete grade and Member type with complete data of three tests*

Grade	Beam	Column	Slab	Total
M20	38	1	25	64
M25	2	8	7	17

NPRC Journal of Multidisciplinary Research
Volume 3, Issue 7, July, 2026 Pages: 17-38
ISSN: 3059-9148 (Online)
DOI: 10.3126/nprcjmr.v3i7.95540

Total	40	9	32	81

All within-stratum correlations are restricted to cells with n> 7 (M20 beam n = 38, M20 slab n = 25, M25 column n = 8, M25 slab n = 7). M20 column (n = 1) and M25 beam (n = 2) are excluded from inferential analyses. Cells with fewer observations are excluded from inferential analyses to prevent sample size bias. However, these minor cell configurations are preserved in the primary dataset for descriptive baseline completeness.

3.3. Non-Destructive Test

The UPV test was carried out by a portable ultrasonic instrument with direct, semi-direct, or indirect probing depending on access availability. Couplant was applied to both sides of the probe and the loose or burnt surface plaster was scraped lightly before conducting any test. Both the type of probing and the distance traversed during probing were noted for each reading. "Readings with velocities below 2.0 km/s, caused by the probe traversing reinforcement or cracks, were discarded. Similarly, the rebound tests were carried out with a Schmidt N hammer, applying the necessary orientation correction factors based on the impact angle relative to the tested structural surfaces. Sixteen rebounds were carried out per element, and their outliers were eliminated to get the member mean rebound number.

3.4. Concrete Core Extraction and Testing

Cores of nominal 67–69 mm diameter were extracted from members on which NDT had already been performed. NDT test grids were positioned on same member faces and regions from which cores were subsequently extracted. However, some places where access constraints prevented exact co-location, the nearest accessible sound surface was used. These minor spatial offset between the exact surface NDT impact points and physical core drill paths is acknowledged as limitation of the field constraints. Sampling was conducted at standardized low-stress zones i.e. at mid-span for beams and slabs and mid-height for columns. While these positions ensure structural safety, fire-induced thermal degradation varies across a member's geometry, typically peaking at beam soffits and exposed column faces. The failure load was determined by applying axial compression following IS 516 Part 4(Bureau of Indian Standards, 2018) , while the equivalent cube compressive strength was determined using the standard length-to-diameter and IS 516 (Bureau of Indian Standards, 2018) correction factors. Strength retention is defined as the ratio of actual core strength to the nominal strength of the design and is expressed as Eq. (*1*)

$$Retention\ (\%) = \frac{f_{ck,core}}{f_{ck,design}} \times 100\% \qquad (1)$$

3.5. Statistical Analysis

Group differences were analysed using a two-tailed Welch t-test with the Welch-Satterthwaite degree of freedom calculated based on the group variances and Mann-Whitney U test as a non-parametric test for robustness. The effect size was quantified using Cohen's d, with values of 0.2, 0.5, and 0.8 representing small, medium, and large effect size, respectively(Cohen, 1988). Correlation of member-level agreement between NDT score and core strength was determined

NPRC Journal of Multidisciplinary Research
Volume 3, Issue 7, July, 2026 Pages: 17-38
ISSN: 3059-9148 (Online)
DOI: 10.3126/nprcjmr.v3i7.95540

using Pearson and Spearman correlation analysis, where 95% confidence interval of Pearson's coefficient was calculated using the Fisher z-transformation method.

Field recalibrated single-method equations were estimated by Ordinary Least Squares (OLS) for each combination of NDT method (UPV, RN) and stratum (Pooled, M20, M25). This results in six distinct empirical models in the form $f_{ck} = \alpha + \beta \times NDT$. For each fit, OLS slope and intercept with 95% confidence intervals (CI), in-sample R^2, Leave-One-Out-Cross-Validated R2 ($R2_{LOOCV}$) to penalise overfitting, and Root Mean Square Error (RMSE) were reported. To test if the slope of the NDT-strength regression differs between grade strata (M20 vs M25), an interaction term (β_3) was included in the regression model $f_{ck} = \beta_0 + \beta_1 \cdot NDT + \beta_2 \cdot I(M25) + \beta_3 \cdot NDT \cdot I(M25)$, where I(M25) is an indicator dummy variable set to 1 for M25 and 0 for the M20 stratum. The null hypothesis $(H_0: \beta_3 = 0)$ was tested against a two-sided alternative to determine the nature of the grade-level effect.

Two specifications in linear and log-bilinear power forms $f_{ck} = a + b.V + c.RN$ and $\ln(f_{ck}) = a + b.\ln(V) + c.\ln(RN)$ were estimated by ordinary least squares for the SonReb combined method analysis. In-sample R^2, leave-one-out cross-validated R^2 (R^2_{LOOCV}), and RMSE metrics were used for evaluating predictive performance. The between-building variability was quantified with the intraclass correlation coefficient (ICC) estimated using one-way random effects ANOVA variance partitioning ($ICC = \frac{\sigma_u^2}{\sigma_u^2 + \sigma_e^2}$), with 95% confidence intervals obtained by cluster bootstrap (1000 iterations, resample buildings with replacement, seed = 42). The effect of building on the relation between NDT and core compressive strength was further assessed by ordinary least-squares regression with building included as a fixed-effect dummy set, which is an equivalent estimator to the random-intercept mixed model for the same fixed-effect specification. A significance level of 0.05 was selected. The analysis was performed in Python 3.13 using pandas, NumPy, and SciPy libraries.

4. Results

4.1. Descriptive NDT and Core response

A summary of the descriptive statistics for all three tests in each member of both grades (M20 and M25) is presented in Table II. The database includes a broad distribution of fire damage. UPV varied between 0.70 km/s for the worst-case damaged M25 column and 4.14 km/s for the least damaged M20 beam, RN varied from 16.9 to 60.5, and core strengths varied between 4.2 MPa and 41.1 MPa, with an average of 17.0 MPa. Distributions of core strength for the four cells containing more than seven samples (n ≥ 7) are depicted in Figure 1.

***Table II**: Descriptive statistics by grade and member type*

Group	n	UPV mean (SD)	RN mean (SD)	Core f_ck (SD)	Retention % (SD)
M20 beam	38	2.86 (0.66)	38.9 (9.3)	15.6 (7.3)	77.9 (36.7)
M20 slab	25	2.81 (0.83)	36.1 (12.1)	15.4 (7.2)	77.1 (36.0)
M20 column	1	2.28 (-)	32.1 (-)	8.9 (-)	44.6 (-)
M25 column	8	3.40 (0.38)	50.1 (1.7)	21.6 (6.7)	86.5 (26.9)

NPRC Journal of Multidisciplinary Research
Volume 3, Issue 7, July, 2026 Pages: 17-38
ISSN: 3059-9148 (Online)
DOI: 10.3126/nprcjmr.v3i7.95540

M25 slab	7	2.65 (1.10)	45.0 (5.6)	30.1 (10.0)	120.3 (40.1)
M25 beam	2	1.45 (1.05)	31.6 (0.6)	10.4 (2.1)	41.6 (8.3)

M20 column (n = 1) and M25 beam (n = 2) are reported for completeness; all inferential analyses are restricted to cells with n ≥ 7. UPV is in km/s, RN dimensionless, core f_{ck} in MPa, retention in % of design strength.

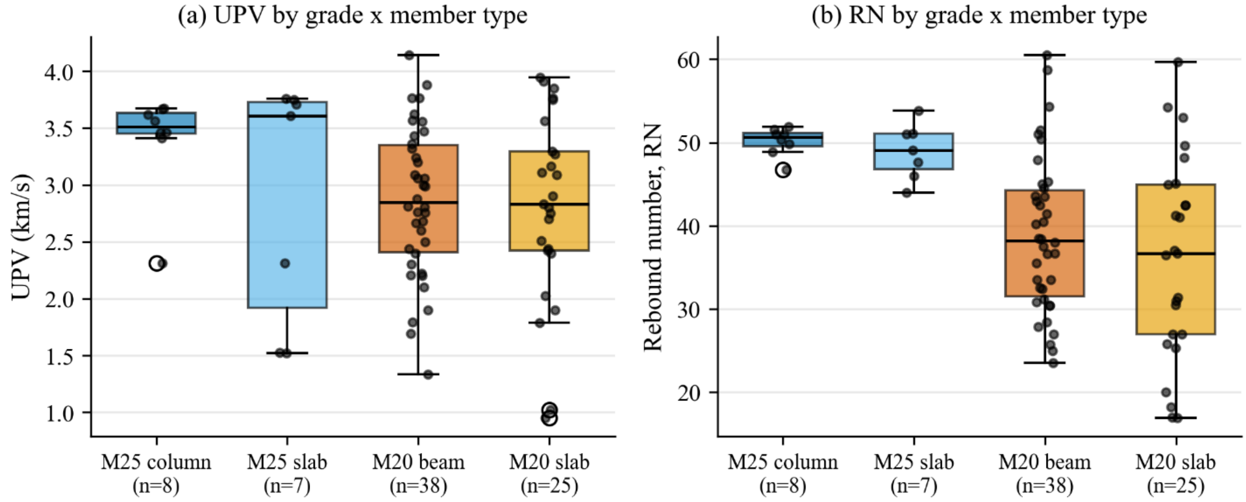

Figure 1: Distribution of (a) UPV readings, and (b) Mean Rebound Number by Concrete Grade and Member type.

4.2. Group Comparisons

Three pairwise group comparisons were conducted on the four cells with n ≥ 7. It constitutes cross-grade (M25 column vs M20 beam) and within-grade, between member type (M25 column vs M25 slab; M20 beam vs M20 slab). Results are summarised in Table III. The cross-grade comparison was clearly significant for both NDT methods. M25 columns showed higher UPV (mean 3.40 vs 2.86 km/s; Welch t (14.2) = 2.81, p = 0.014; Mann-Whitney U = 231.0, p = 0.021; Cohen's d = 0.85), substantially higher RN (50.1 vs 38.9; t (43.8) = 6.93, p < 0.0001; U = 264.0, p = 0.0012; d = 1.31), and higher residual core strength (21.6 vs 15.6 MPa; t (10.4) = 2.17, p = 0.054; U = 229.0, p = 0.027; d = 0.83).

***Table III**: Two-sample comparisons between groups (Welch t-test and Mann-Whitney U)*

Comparison	**Measure**	**n_1**	**n_2**	**Mean n_1**	**Mean n_2**	**Diff.**	**t**	**df**	**p (t)**	**Cohen's d**	**U**	**p (MW)**
M25 col vs M20 beam	UPV	8	38	3.40	2.86	0.54	2.81	14.2	0.014	0.85	231.0	0.021
M25 col vs M20 beam	RN	8	38	50.1	38.9	11.3	6.93	43.8	< 0.0001	1.31	264.0	0.0012

M25 col vs M20 beam	Core	8	38	21.6	15.6	6.0	2.17	10.4	0.054	0.83	229.0	0.027
M25 col vs M25 slab	UPV	8	7	3.40	2.88	0.51	1.19	7.9	0.27	0.65	26.5	0.91
M25 col vs M25 slab	RN	8	7	50.1	48.9	1.20	0.86	8.6	0.42	0.46	34.0	0.52
M25 col vs M25 slab	Core	8	7	21.6	30.7	-9.1	-2.09	11.2	0.060	-1.11	11.0	0.054
M20 beam vs M20 slab	UPV	38	25	2.86	2.81	0.05	0.26	43.4	0.80	0.07	473.5	0.99
M20 beam vs M20 slab	RN	38	25	38.9	36.1	2.8	0.97	42.0	0.34	0.26	538.0	0.38
M20 beam vs M20 slab	Core	38	25	15.6	15.4	0.2	0.08	49.0	0.94	0.02	481.5	0.93

The two within-grade comparisons told different stories. M20 beam vs M20 slab was non-significant on every measure ($p \geq 0.34$ throughout), indicating that the two horizontal M20 member types behave similarly under the fire exposure in this dataset. Conversely, M25 column vs M25 slab showed a notable decoupling: UPV and RN did not separate the two groups (UPV: $p = 0.27$; RN: $p = 0.42$), yet destructive core strength differed by 9.1 MPa with the M25 slabs averaging higher (30.7 vs 21.6 MPa; $t\ (11.2) = -2.09$, $p = 0.060$; $U = 11.0$, $p = 0.054$; $d = -1.11$). This physical divergence is clearly shown in the box plots of Figure 2, where the M25 slab data blocks sit distinctly higher than the corresponding column data. Large differences in residual core strength that NDT readings do not detect are a direct demonstration of NDT's limited absolute discrimination within the high-strength stratum and motivate the more detailed agreement analysis in Section 4.5.

NPRC Journal of Multidisciplinary Research
Volume 3, Issue 7, July, 2026 Pages: 17-38
ISSN: 3059-9148 (Online)
DOI: 10.3126/nprcjmr.v3i7.95540

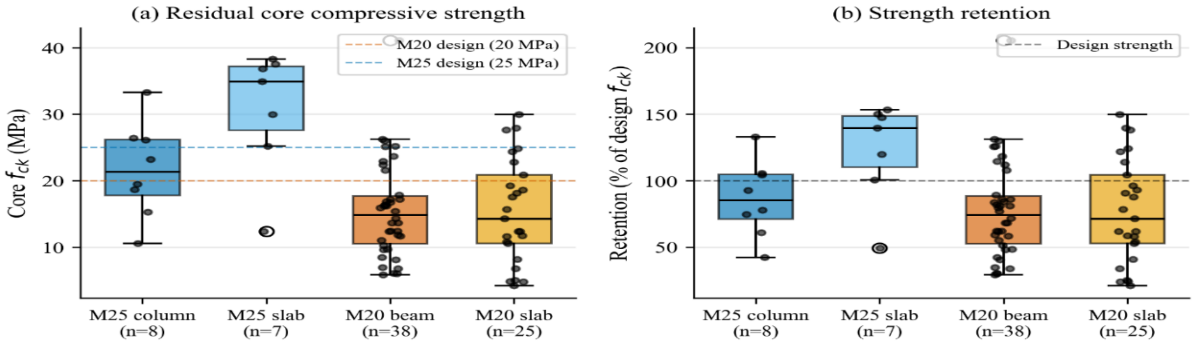

Figure 2: (a) Residual Core strength and (b) Strength retention (% of design f_{ck}) by Concrete Grade and member type.

4.3. Member Level Correlation between NDT and Core

Both NDT methods correlated significantly with destructive core strength across the full sample (Table IV, Figure 3). UPV showed a moderately strong positive correlation with core strength (Pearson r = +0.64, $R^2 = 0.40$, $p < 0.0001$), and the rebound number showed a stronger correlation (r = +0.72, $R^2 = 0.52$, $p < 0.0001$). Spearman rank correlations were closely consistent with the Pearson estimates (ρ = +0.69 for UPV; ρ = +0.78 for RN), supporting robustness against non-linearity. The two NDT methods were also correlated with one another (r = +0.63, $p < 0.0001$). Within the M20 stratum, which contains 64 of the 81 members and dominates the inference, both correlations were stronger (UPV and Core: r = +0.68; RN and Core r = +0.78). Within the M25 stratum (n = 17), the two methods diverged. UPV remained significantly correlated with core strength (r = +0.64, p = 0.0058), but RN was not (r = +0.32, p = 0.21). The Section 4.2 finding that M25 columns and M25 slabs differ substantially in residual core strength without a matching difference in either NDT reading explains this collapse directly: the M25 slabs combine lightly-damaged interiors with only moderate rebound surfaces, so the within-M25 RN signal does not track strength. This pattern is consistent with the literature observation that the rebound hammer becomes insensitive to bulk strength once the surface layer is intact (Kowalski & Wróblewska, 2018; Wróblewska & Kowalski, 2020), and it reinforces the central finding that RN is unsafe as an absolute predictor for high-strength damaged concrete.

Table IV*: Pearson Correlation between NDT response and destructive core strength, with Spearman ρ as robustness check.*

Relationship	Group	n	Pearson r	95% CI	R²	p	Spearman ρ	p (ρ)
UPV vs Core	All members	81	+0.64	[+0.48, +0.75]	0.40	< 0.0001	+0.69	< 0.0001
UPV vs Core	M20 stratum	64	+0.68	[+0.52, +0.79]	0.46	< 0.0001	+0.70	< 0.0001
UPV vs Core	M25 stratum	17	+0.64	[+0.23, +0.86]	0.41	0.0058	+0.78	0.00024

NPRC Journal of Multidisciplinary Research
Volume 3, Issue 7, July, 2026 Pages: 17-38
ISSN: 3059-9148 (Online)
DOI: 10.3126/nprcjmr.v3i7.95540

RN vs Core	All members	81	+0.72	[+0.60, +0.81]	0.52	< 0.0001	+0.78	< 0.0001
RN vs Core	M20 stratum	64	+0.78	[+0.66, +0.86]	0.61	< 0.0001	+0.82	< 0.0001
RN vs Core	M25 stratum	17	+0.32	[−0.19, +0.70]	0.10	0.21	+0.06	0.81
UPV vs RN	All members	81	+0.63	[+0.48, +0.75]	0.40	< 0.0001	+0.63	< 0.0001

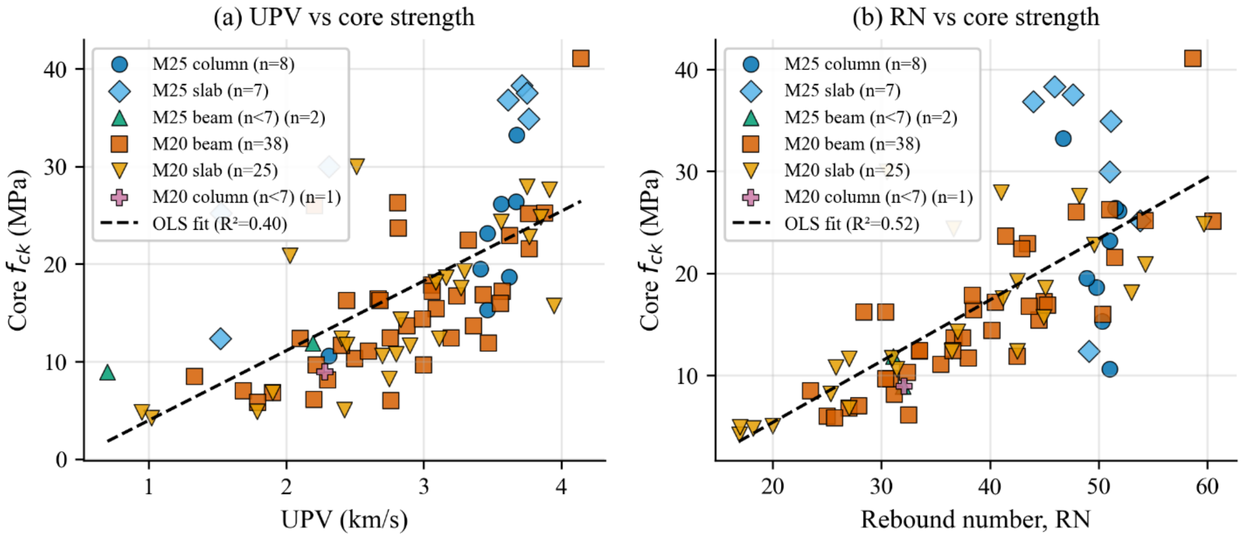

Figure 3: Member-level Scatter Plot of (a) UPV and (b) RN against Destructive Core strength

4.4. Field Recalibrated Single-method Equations

The six distinct empirical models are summarised in

Table V and visualised in Figure 4. In the case of UPV, the three fits have similar slopes (7.16 for pooled, 7.04 for M20 and 6.22 for M25) with overlapping 95% confidence intervals. The pooled UPV equation Eq. (2) achieved $R^2 = 0.4$ with R^2_{LOOCV}=0.37. However, the M20 stratum equation Eq. (3) improved cross-validated fit to R^2_{LOOCV}= 0.43 with RMSE 5.43 MPa. The M25 stratum equation Eq. (4) had similar in-sample R^2 (0.41) but a notably lower R^2_{LOOCV} (0.27), reflecting the smaller sample (n = 17) and consequent overfitting.

$$\text{UPV pooled (n=81):} \quad f_{ck} = 7.16 \cdot V - 3.20 \qquad (2)$$

$$\text{UPV M20 (n=64):} \quad f_{ck} = 7.04 \cdot V - 4.49 \qquad (3)$$

$$\text{UPV M25 (n=17):} \quad f_{ck} = 6.55 \cdot V + 4.71 \qquad (4)$$

In the case of Rebound number, the three fits showed a more dramatic pattern. The pooled RN equation Eq. (5) has $R^2 = 0.52$ with $R^2_{LOOCV} = 0.50$ and RMSE 6.02 MPa. For the M20 stratum, the fit was improved with $R^2 = 0.61$, $R^2_{LOOCV} = 0.59$, RMSE 4.61 MPa (Eq.(6)). However, in

NPRC Journal of Multidisciplinary Research
Volume 3, Issue 7, July, 2026 Pages: 17-38
ISSN: 3059-9148 (Online)
DOI: 10.3126/nprcjmr.v3i7.95540

the M25 stratum (Eq. (7)), the rebound equation degraded with $R^2 = 0.10$, $R^2_{LOOCV} = -0.12$, with slope confidence interval crossing zero value, i.e. [-0.31, +1.31]. A negative cross-validated R^2 indicates that the stratum-specific fit predicts worse than the M25 sample mean alone. It confirms that the within M25 rebound data does not track residual strength, consistent with the Section 4.2 finding that M25 columns and slabs differ in residual strength without matching RN differences.

RN pooled (n=81): $f_{ck} = 0.60 \cdot R - 6.62$ (5)

RN M20 (n=64): $f_{ck} = 0.56 \cdot R - 5.58$ (6)

RN M25 (n=17): $f_{ck} = 0.50 \cdot R + 0.20$ (7) (Not recommended for use)

***Table V**: Field recalibrated single-method equations at three stratification levels*

NDT	Stratum	n	Slope β	95% CI on β	Intercept α	R²	R^2_{LOOCV}	RMSE (MPa)
UPV	Pooled	81	+7.16	[+5.21, +9.10]	−3.20	0.40	0.37	6.72
UPV	M20	64	+7.04	[+5.11, +8.96]	−4.49	0.46	0.43	5.43
UPV	M25	17	+6.55	[+2.21, +10.89]	+4.71	0.41	0.27	7.51
RN	Pooled	81	+0.60	[+0.47, +0.73]	−6.62	0.52	0.50	6.02
RN	M20	64	+0.56	[+0.45, +0.67]	−5.58	0.61	0.59	4.61
RN	M25	17	+0.50	[−0.31, +1.31]	+0.20	0.10	−0.12	9.24

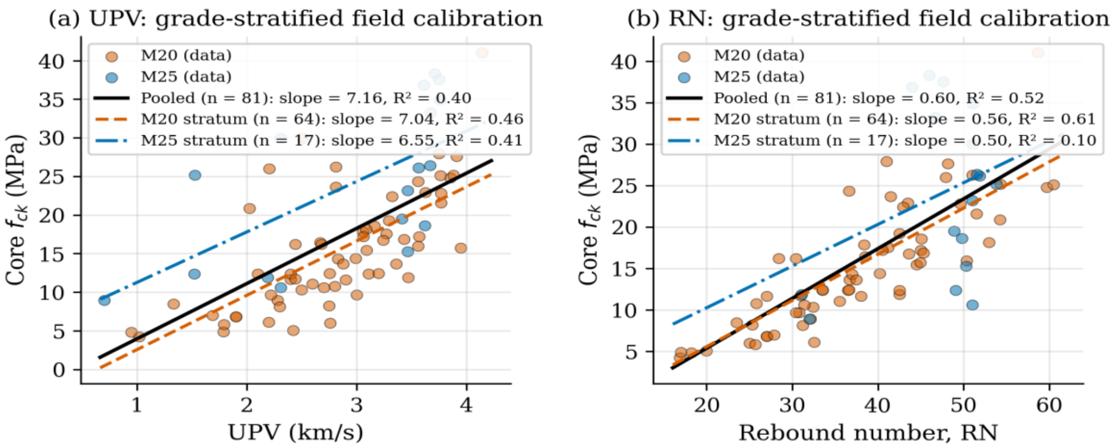

Figure 4: Field recalibrated single-method equations by grade stratum (a) UPV (b) Rebound Number

NPRC Journal of Multidisciplinary Research
Volume 3, Issue 7, July, 2026 Pages: 17-38
ISSN: 3059-9148 (Online)
DOI: 10.3126/nprcjmr.v3i7.95540

The interaction term β_3 was used to check if the slope differs between the two grades. For UPV, $\beta_3 = -0.49$ (95% CI [−4.23, +3.25]; p = 0.794), showing that slopes are statistically equivalent between the two strata. In the case of RN, $\beta_3 = -0.054$ (95% CI [−0.54, +0.43]; p = 0.825), with the same result. It shows that one unit increase in either UPV or Rebound Number reflects the same rate of strength increase in both M20 and M25 fire-damaged concrete. The difference between the two grades is an intercept shift in strength. However, the analysis notes a practical challenge within the M25 concrete group. Localised variations in Rebound Number readings do not reliably track individual core strength variations due to high data dispersion in the stratum.

4.5. Son-Reb Combined Method Analysis

The combination of UPV and the rebound number (SonReb) is suggested to fix some limits of using those methods alone (El-Mir et al., 2023). Two SonReb versions were checked against a full set, viz. linear combination ($f\_ck = a + b.V + c.RN$), and a log-bilinear power form. These were analysed with Ordinary least squares on n = 81 samples. Evaluation was done with in-sample R^2, Leave-One-Out Cross-Validated R^2 (R^2_{LOOCV}), and RMSE on the MPa scale. The results are summarised in Table VI and visualised in Figure 5.

***Table VI**: SonReb combined-method linear regressions at three stratification levels, compared with the single-method linear regressions*

Form	Stratum	n	Equation	R^2	R^2_LOOCV	RMSE (MPa)
Single UPV	Pooled	81	$f_{ck} = 7.16 \cdot V - 3.20$	0.40	0.37	6.72
Single RN	Pooled	81	$f_{ck} = 0.60 \cdot R - 6.62$	0.52	0.50	6.02
SonReb linear	Pooled	81	$f_{ck} = -9.98 + 3.36 \cdot V + 0.443 \cdot R$	0.58	0.54	5.67
SonReb linear	M20	64	$f_{ck} = -7.57 + 2.23 \cdot V + 0.442 \cdot R$	0.63	0.60	4.49
SonReb linear	M25	17	$f_{ck} = +0.19 + 6.24 \cdot V + 0.114 \cdot R$	0.41	0.14	7.48
SonReb power	Pooled	81	$f_{ck} = 0.111 \cdot V$^0.379$\cdot R$^1.243	0.56	0.54	5.77

$$f_{ck} = -9.98 + 3.36\,V + 0.443\,RN \qquad (8)$$

$$f_{ck} = 0.111 \times V^{0.379} \times RN^{1.243} \qquad (9)$$

Both SonReb forms did better than a single-method linear regression. For the linear SonReb formula Eq. (8), it had the best in-sample and cross-validated fits ($R^2 = 0.58$, R^2LOOCV = 0.54, RMSE = 5.67 MPa). This improved upon the single-method RN regression by about four percentage points in cross-validated R^2 and reduced the RMSE by approximately 6%. The power form Eq. (9) also performed similarly ($R^2 = 0.56$, $R^2_{LOOCV} = 0.54$). After stratifying the

NPRC Journal of Multidisciplinary Research
Volume 3, Issue 7, July, 2026 Pages: 17-38
ISSN: 3059-9148 (Online)
DOI: 10.3126/nprcjmr.v3i7.95540

linear SonReb fit by Concrete grade as shown in Table VI shows similar pattern as observed in single-method analysis. M20 stratum fit was the best on cross-validated R^2 of 0.60; the pooled fit was intermediate (0.54), and M25 stratum fit overfitted heavily (R2= 0.41) in sample but R^2_{LOOCV} = 0.14. Figure 5 shows that predictions match the 1:1 line for most of the M20 values, but flatten out for higher strength values above 30 MPa

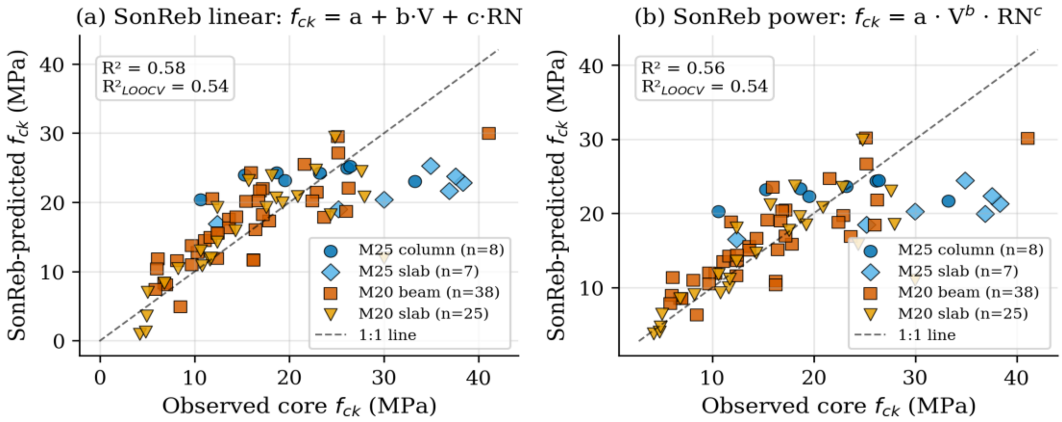

Figure 5 : Pooled SonReb predicted vs observed residual core strength: (a) linear form (Eq. 9); (b) power form (Eq. 10).

4.6. Between building variability

Around 63% of the total variance in core compressive strength is due to differences between buildings (ICC = 0.63, 95% bootstrap CI 0.24 - 0.82; σ_u^2 = 50.7, σ_e^2 = 30.2). In Figure 6, each building has a unique average strength range, from highly damage value around 7 MPa to those low-damage buildings with averages above 36 MPa. The analysis was done to account for unique site differences among buildings. After accounting for such building-level variations, the rebound number remained the most reliable predictor of core compressive strength (standardised β = +0.35, p = 0.0026). In contrast, the effect of UPV became weaker and was no longer statistically significant. Also, the nominal concrete grade or the specific member type offered no useful predictive value ($p \geq 0.07$ in all cases). The model's R^2 jumped from 0.69 for pooled baseline regression to within-building R^2 of 0.78 after accounting for building-level

NPRC Journal of Multidisciplinary Research
Volume 3, Issue 7, July, 2026 Pages: 17-38
ISSN: 3059-9148 (Online)
DOI: 10.3126/nprcjmr.v3i7.95540

fixed effects. It confirms that controlling for the building (such as a fire event) sharpens the within-building relationship between NDT and Core without changing its sign or direction.

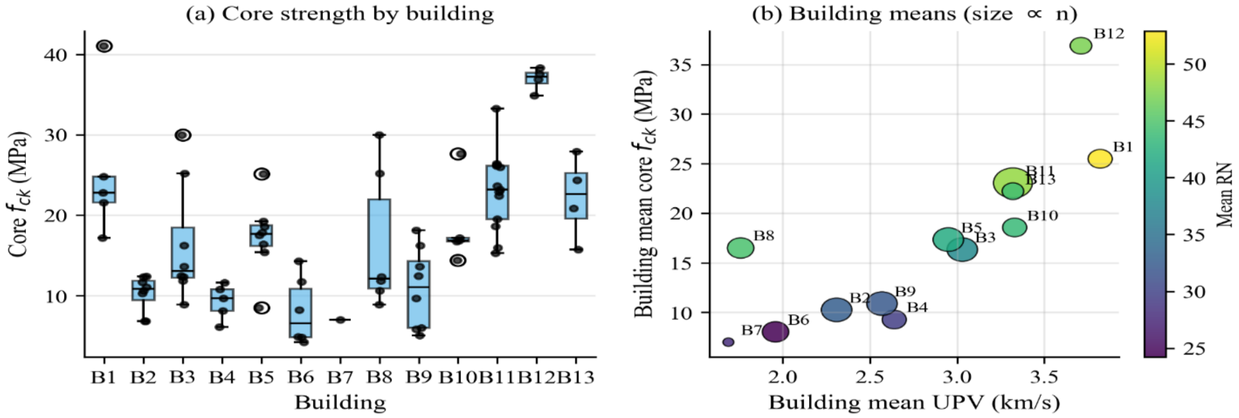

Figure 6: Between-building variability (a)Core Compressive strength varies between 13 study buildings (b) Building-level mean UPV vs. Mean Core strength

5. Discussion

5.1. Necessity of Field Calibration and Model Non-transferability

The comparative review of the empirical NDT-to-strength calibrations that there is no transferable closed-form equation resulting from the NDT-to-strength literature(Pucinotti, 2015; Wróblewska & Kowalski, 2020). Individual empirical calibrations vary dramatically in their mathematical form, slope, intercept, and underlying population. These differences arise from intrinsic characteristics of NDT measurements such as the integration of both surface and bulk properties over an area whose mechanics depend heavily on material composition, environment, etc. This shows the requirement of recalibration against destructive core samples from the same structures in any postfire assessment. Consequently, the field-calibrated equations derived here cannot be interpreted as a new universal formula. On the contrary, the statistical recalibration equation serves two distinct purposes. First, it provides a statistically defensible baseline estimate for engineers needing to derive a localised calibration based on a few core samples. Second, it provides an overall standard for the evaluation of such project-specific calibrations of M20 and M25 fire-damaged RC structures in Nepal.

5.2. Evaluation of Pooled Vs. Stratified Models: Insights from Slope-Equality Testing

One important observation from this statistical analysis is the non-significance of the difference in the slope of the regression line of NDT versus strength within both M20 and M25 concrete strata. This can be visually observed in Figure 4, where both regression lines for each type of NDT measurement (UPV and RN) are almost parallel to each other. The main difference that arises between the two strata is in their intercepts. This implies that while the concrete grade determines the strength intercept for any given NDT, the slope of the strength regression per unit NDT increment is the same for both grades.

NPRC Journal of Multidisciplinary Research
Volume 3, Issue 7, July, 2026 Pages: 17-38
ISSN: 3059-9148 (Online)
DOI: 10.3126/nprcjmr.v3i7.95540

From a calibration point of view, a pooled slope may actually be a reliable estimator of both grades provided an intercept adjustment for each grade is made. Nevertheless, an important caution should be raised regarding the Rebound Number model. Even though there was no statistically significant difference found in the interaction test β_3 concerning the RN slope, stratified analyses presented in Table V show that the RN model for M25 completely degrades (R^2=0.10, R^2_{LOOCV}= -0.12), and the CI for slope includes zero (-0.31,+1.31). A negative cross-validated R^2 indicates that a stratum-specific regression model performs worse than simply using the M25 sample mean alone.

Despite the M25 stratum showing considerable variation in true core compressive strength values (10 MPa to 41 MPa), the corresponding surface rebound values are distributed in a relatively compact range of high values (mean values between 45.0 and 50.1). This may have occurred because of possible rapid cooling or vitrification of the surface layer, making it superficially intact. However, the inner bulk concrete experiences significant degradation due to heat, which the rebound hammer fails to capture. Hence, the apparent equality of slopes in the interaction analysis is not evidence of reliable relationship sharing, but rather a result of high variability and limited sample sizes of M25 stratum members. So, it implies that developing a reliable stratum-based equation for predicting compressive strength of M25 and higher grades of fire-damaged concrete necessitates obtaining more fire damaged sample size than the current dataset provides. Also, the use of standalone RN equations should be avoided for M25 post-fire assessments. One should prioritise UPV or combined SonReb specifications, verified by core extraction for higher grades.

5.3. Combined SonReb Analysis and Multi-variable predictive performance

The combined SonReb approach clearly offers its advantages by integrating the complementary physical characteristics of both NDT approaches. The pooled linear SonReb regression Eq. (8) provided an in-sample R^2 of 0.58 and cross-validated R^2_{LOOCV} of 0.54. It signifies a relatively small but significant gain of around four percentage points over the pooled RN-only model and a substantially higher 17 percentage point gain over the pooled UPV-only model. These results are consistent with the well-established literature that the combination of both techniques helps balance out the surface-layer effect inherent in the rebound hammer technique against the bulk-path effect of ultrasonic wave propagation(Pucinotti, 2015; Qasrawi, 2000) . In particular, the stratified linear M20-stratum SonReb regression provided the highest level of predictive accuracy among all models considered in this analysis, R^2_{LOOCV} = 0.60, RMSE = 4.49MPa. As a result, when the sample size of low-grade concrete is sufficiently large, this stratified model represents the most reliable choice for forensic post-fire evaluations. While the M25-stratum SonReb regression suffered from very severe overfitting, resulting in an in-sample R^2 of 0.41 while producing only R^2_{LOOCV}= 0.14. In essence, this poor performance is the result of the mathematical problem of estimating the value of three different regression parameters $(\alpha, \beta_1, \beta_2)$based on a very small number of observations (only 17 samples). Also, the scatter plot of predicted vs. actual values of the pooled SonReb exhibit a flattening effect when the strength exceeds 30MPa. The reason for this lies in the fact that the SonReb model has a heavy

NPRC Journal of Multidisciplinary Research
Volume 3, Issue 7, July, 2026 Pages: 17-38
ISSN: 3059-9148 (Online)
DOI: 10.3126/nprcjmr.v3i7.95540

reliance on the rebound coefficient $\beta_2 = 0.443$, making the blind classification of M25 surface rebound measurements lead to biased results. So, the pooled SonReb equation cannot be safely recommended as a default baseline for M25 elements. In higher-grade post-fire assessments, the SonReb approach must either be calibrated using a larger sample size or be used along with comprehensive core extraction.

5.4. Between Building variability as the dominant source of calibration uncertainty

The variance partitioning analysis has shown that nearly 63% of the overall variance of the core strength is due to between-buildings differences (ICC = 0.63, 95% CI [0.24,0.82]). Hence, it can be concluded that the concrete degradation results are driven mainly by the properties of the macro environment at the time of the fire, such as fuel loads in particular areas, time of exposure to fire, ventilation, and maximum attained temperatures(Kodur & Agrawal, 2016; Qin et al., 2022). The effect of building-level variation is overwhelmingly more substantial than that of within-building variation such as concrete grade and element type ($p \geq 0.07$).

After accounting for between-building variation using the fixed effects dummy variable set, the variance of core strength explained by the model was greatly increased. The within-building R^2 grew from 0.69 to 0.78. In this controlled framework, the Rebound Number remained the most reliable and statistically significant predictor of core strength (standardized β = +0.35, p=0.0026). However, the contribution made by the UPV measure was weakened and became insignificant. It means that within a given fire-damaged building, local differences in surface hardness provide a good indicator of the core strength for each component, whereas UPV measures play a minor role in this respect.

This observation is highly relevant to the field application procedures of fire damage assessment. NDT methods are extremely effective at distinguishing highly damaged members from less damaged ones in a specific fire-damaged building structure. Nonetheless, the raw data empirical equations presented in this work cannot simply be applied to a totally new building where fire behaviour differs from the baseline average in our data.

Consequently, when utilising the above empirical models for an assessment of another post-fire structure, caution should be exercised. In fact, such empirical models should not be considered as direct predictors of absolute results. First of all, the assessment should be started by extracting a modest sample of destructive control cases, which serves to calculated building specific intercept shift. Then, localised NDT equations can be used to scan, rank and predict the strength of remaining elements.

6. Limitations

Some of the the limitations of the study are as follows. Firstly, the dataset is predominantly represented by the M20 members (64 out of 81; 79.0%). The M25 results have been obtained using 17 M25 members spread over three cell types (M25 column, n=8; M25 slab, n=7; M25 beam, n=2). The correlation coefficients as well as the breakdown within M25 of the rebound regression are best interpreted as characteristics of the M25 population represented in the current dataset. Furthermore, the results of the within-M25 breakdown, especially the negative

NPRC Journal of Multidisciplinary Research
Volume 3, Issue 7, July, 2026 Pages: 17-38
ISSN: 3059-9148 (Online)
DOI: 10.3126/nprcjmr.v3i7.95540

R^2_{LOOCV} coefficient in the RN stratum fit, must be confirmed in a larger high-strength sample. The M25 RN failure may be specific to this dataset's distribution of damage types and should be replicated in a larger M25-only sample.

Secondly, the off-diagonal cells in the M20 column (n=1) and M25 beam (n=2) do not contain sufficient data for statistical inference and were thus excluded from Table III-Table VI, while included in Table II for consistency. Thirdly, there is no instrumental measure of fire temperatures, fire duration, and fire-load density for any of the buildings studied. Finally, the field calibrations of the equations generated above apply to OPC concretes having M20 and M25 grades that have been subjected to post-fire condition tests in Nepal. Their applicability to other grades, other aggregate sources, or undamaged concrete is not implied and should be verified against site-specific cores before use.

7. Conclusion

The present investigation evaluated the reliability of Non-Destructive Testing (NDT) using Ultrasonic Pulse Velocity (UPV), Rebound Hammer (RN), and SonReb models in 81 reinforced concrete elements that have suffered from fires in 13 buildings located in Nepal. The main conclusions drawn from this analysis can be summarized as follows:

1. Both UPV and RN provide strong correlation coefficients (r = +0.64 and +0.72, respectively), but existing standard NDT codes tend to overestimate residual concrete strength in fire-damaged elements. Project-specific destruction cores should be obtained for calibration purposes.
2. The results of variance partitioning showed that approximately 63% of the variability of residual core strength (ICC = 0.63) depends on macro-level factors such as building-specific fire properties (peak temperature, fire exposure, etc.) instead of within-building parameters like member type and concrete class. Thus, it will be impossible to transfer the NDT model across different fires due to significant building-specific biases.
3. The interaction test showed that the slopes of the NDT vs. strength regression are statistically identical in M20 and M25 mixes ($p \geq 0.79$). The key variation occurs through the difference in intercepts reflecting the nominal design strength. For buildings made with different mixes, using a common slope and stratifying on intercepts leads to a workable procedure and sound statistical justification for field calibration.
4. M25 rebound regression failed in its cross-validation step with R^2_{LOOCV} = -0.12 performing worse than the M25 sample mean. This statistical failure reflects a different effect of fire-induced damage on the bulk interior of the M25 structures than the surface layers. Crucially, UPV did not show this degradation, maintaining a stable and statistically significant tracking of internal damage within M25 stratum.
5. The stratified M20 SonReb linear model provided the most stable predictive framework out of all frameworks tested (R^2_{LOOCV} = 0.60, RMSE = 4.49 MPa), counterbalancing the measurement error from both surface and bulk tests. On the other hand, multi-

NPRC Journal of Multidisciplinary Research
Volume 3, Issue 7, July, 2026 Pages: 17-38
ISSN: 3059-9148 (Online)
DOI: 10.3126/nprcjmr.v3i7.95540

variable SonReb predictions are highly over-fitted, especially when applied to small high-strength samples (n = 17). For M25 members, the pooled SonReb equation is preferred rather than the M25-stratum SonReb as it was heavily overfitted (R^2_{LOOCV} = 0.14).

Overall, NDT methods in post-fire assessment are suitable only for sorting damaged structures and ranking relative member strengths. Quantitative strength estimation for rating purposes will have to depend on a local, building-specific, destructive coring method to reduce between-building variability by 63%

Ethical and Scholarly Compliance

This investigation did not involve human participants or animal subjects. Hence, formal institutional ethical approval was not required for the structural testing protocols. All field non-destructive testing (NDT) and destructive core extractions across the investigated building sites were conducted following required permissions and clearances secured from the respective building owners.

Transparency Statement: The authors confirm that this study has been conducted with honesty and in full adherence to ethical guidelines.

Funding: The study received no external funding.

Conflict of Interest: The authors declare there is no conflict of interest.

NPRC Journal of Multidisciplinary Research
Volume 3, Issue 7, July, 2026 Pages: 17-38
ISSN: 3059-9148 (Online)
DOI: 10.3126/nprcjmr.v3i7.95540

References

Agrawal, A., & Kodur, V. K. R. (2020). A Novel Experimental Approach for Evaluating Residual Capacity of Fire Damaged Concrete Members. *Fire Technology*, *56*(2), 715-735. https://doi.org/10.1007/s10694-019-00900-1

Bungey, J. H., Millard, S. G., & Grantham, M. G. (2006). *Testing of Concrete in Structures (4th ed., 352 pp.)*. Taylor & Francis.

Bureau of Indian Standards. (1992a). Non-destructive testing of concrete — Methods of test, Part 1: Ultrasonic pulse velocity. In *IS 13311 (Part 1)*. New Delhi: Bureau of Indian Standards.

Bureau of Indian Standards. (1992b). Non-destructive testing of concrete — Methods of test, Part 2: Rebound hammer. In *IS 13311 (Part 2)*. New Delhi: Bureau of Indian Standards.

Bureau of Indian Standards. (2018). Methods of tests for strength of concrete — Part 4: Cored specimens. In *IS 516 (Part 4)*. New Delhi: Bureau of Indian Standards.

Caetano, H., Ferreira, G., Rodrigues, J. P. C., & Pimienta, P. (2019). Effect of the high temperatures on the microstructure and compressive strength of high strength fibre concretes. *Construction and Building Materials*, *199*, 717-736. https://doi.org/10.1016/j.conbuildmat.2018.12.074

Choi, Y., Kang, J.-W., Hwang, T.-Y., & Cho, C.-G. (2021). Evaluation of residual strength with ultrasonic pulse velocity relationship for concrete exposed to high temperatures. *Advances in Mechanical Engineering*, *13*(9), 16878140211034992. https://doi.org/10.1177/16878140211034992

Cohen, J. (1988). *Statistical Power Analysis for the Behavioral Sciences (2nd ed., 567 pp.)*. Lawrence Erlbaum Associates. https://doi.org/https://doi.org/10.4324/9780203771587

Colombo, M., & Felicetti, R. (2007). New NDT techniques for the assessment of fire-damaged concrete structures. *Fire Safety Journal*, *42*(6), 461-472. https://doi.org/https://doi.org/10.1016/j.firesaf.2006.09.002

Concrete Society. (2008). *Assessment, design and repair of fire-damaged concrete structures (Report No. TR68)*.

El-Mir, A., El-Zahab, S., Sbartaï, Z. M., Homsi, F., Saliba, J., & El-Hassan, H. (2023). Machine learning prediction of concrete compressive strength using rebound hammer test. *Journal of Building Engineering*, *64*, 105538. https://doi.org/10.1016/j.jobe.2022.105538

Elsanadedy, H. M. (2019). Residual Compressive Strength of High-Strength Concrete Exposed to Elevated Temperatures. *Advances in Materials Science and Engineering*, *2019*(1), 6039571. https://doi.org/10.1155/2019/6039571

Felicetti, R. (2006). The drilling resistance test for the assessment of fire damaged concrete. *Cement and Concrete Composites*, *28*(4), 321-329. https://doi.org/https://doi.org/10.1016/j.cemconcomp.2006.02.009

Katuwal, T. B. (2019). Correlation between Concrete Compressive Strength and Rebound Number of River Bed and Crusher Run Coarse Aggregate in Pokhara Valley. *Technical Journal*, *1*(1), 29-33. https://doi.org/10.3126/tj.v1i1.27584

Khoury, G. A. (2000). Effect of fire on concrete and concrete structures. *Progress in Structural Engineering and Materials*, *2*(4), 429-447. https://doi.org/https://doi.org/10.1002/pse.51

NPRC Journal of Multidisciplinary Research
Volume 3, Issue 7, July, 2026 Pages: 17-38
ISSN: 3059-9148 (Online)
DOI: 10.3126/nprcjmr.v3i7.95540

Kodur, V. (2014). Properties of Concrete at Elevated Temperatures. *International Scholarly Research Notices*, *2014*(1), 468510. https://doi.org/https://doi.org/10.1155/2014/468510

Kodur, V. K. R., & Agrawal, A. (2016). An approach for evaluating residual capacity of reinforced concrete beams exposed to fire. *Engineering Structures*, *110*, 293-306. https://doi.org/10.1016/j.engstruct.2015.11.047

Kowalski, R., & Wróblewska, J. (2018). Application of a Sclerometer to the Preliminary Assessment of Concrete Quality in Structures After Fire. *Archives of Civil Engineering*, *64*, 171-186. https://doi.org/10.2478/ace-2018-0069

Liu, C., & Chen, J. (2022). High Temperature Degradation Mechanism of Concrete with Plastering Layer. *Materials*, *15*, 398. https://doi.org/10.3390/ma15020398

Miao, K., Pan, Z., Chen, A., & Timothy, J. J. (2026). A multiscale micromechanical model for high-temperature effects in cementitious materials: From microstructural evolution to macroscopic deterioration. *Cement and concrete research*, *206*, 108264. https://doi.org/https://doi.org/10.1016/j.cemconres.2026.108264

Pasztetnik, M., & Wróblewski, R. (2021). A Literature Review of Concrete Ability to Sustain Strength after Fire Exposure Based on the Heat Accumulation Factor. *Materials*, *14*(16), 4719.

Proceq, S. A. (2019). *Schmidt Hammer: Operating Instructions and Calibration Charts (Type N)* [Manufacturer Technical Manual].

Pucinotti, R. (2015). Reinforced concrete structure: Non destructive in situ strength assessment of concrete. *Construction and Building Materials*, *75*, 331-341. https://doi.org/10.1016/j.conbuildmat.2014.11.023

Qasrawi, H. (2000). Concrete strength by combined nondestructive methods - Simply and reliably predicted. *Cement and concrete research*, *30*, 739-746. https://doi.org/10.1016/S0008-8846(00)00226-X

Qin, D., Gao, P., Aslam, F., Sufian, M., & Alabduljabbar, H. (2022). A comprehensive review on fire damage assessment of reinforced concrete structures. *Case Studies in Construction Materials*, *16*, e00843. https://doi.org/10.1016/j.cscm.2021.e00843

Rashid, K., & Waqas, R. (2017). Compressive strength evaluation by non-destructive techniques: An automated approach in construction industry. *Journal of Building Engineering*, *12*. https://doi.org/10.1016/j.jobe.2017.05.010

Rovnanik, P. (2015). Effect of the aggregate type on the properties of alkali-activated slag subjected to high temperatures. *Materiali in tehnologije*, *49*, 709-713. https://doi.org/10.17222/mit.2014.116

Wróblewska, J., & Kowalski, R. (2020). Assessing concrete strength in fire-damaged structures. *Construction and Building Materials*, *254*, 119122. https://doi.org/10.1016/j.conbuildmat.2020.119122